

Cite this: *RSC Adv.*, 2018, 8, 28533Received 20th April 2018  
Accepted 1st August 2018

DOI: 10.1039/c8ra03384f

rsc.li/rsc-advances

# Photophysical behaviour of BODIPY-phenylacetylene macrocyclic dyads for light-harvesting applications†

Muhammad Yousaf,<sup>ab</sup> Ximena Zarate,<sup>c</sup> Eduardo Schott,<sup>d</sup> Alan J. Lough<sup>e</sup> and Bryan D. Koivisto<sup>id</sup>\*<sup>a</sup>

The synthesis and study of a family of BODIPY-phenylacetylene macrocycles where donor groups have been added to the macrocycle in order to tune the physicochemical properties and absorption profile is reported. Energy transfer is observed between this phenylacetylene antennae and BODIPY core and fluorescence emission from the BODIPY, at any excitation wavelength, is consistent with energy transfer from the macrocycle.

## Introduction

Owing to their rigidity and minimal degrees of conformational freedom, shape-persistent phenylacetylene macrocycles (**1**; Fig. 1) have attracted much attention in supramolecular chemistry and materials science.<sup>1–4</sup> Their extended  $\pi$ -structures are responsible for intense light absorption, and have been explored in a number of optoelectronic and light-harvesting applications.<sup>5</sup> The molecular architecture of large macrocycles with well-defined geometries possesses similarity to natural light harvesting complexes which can absorb light and transfer energy through excitation energy transfer (EET) processes.<sup>6,7</sup> Increasing interest in  $\pi$ -conjugated macrocycles is attributed to their promising application in material science,<sup>8</sup> host-guest systems,<sup>9</sup> storage devices,<sup>10</sup> digital computation,<sup>11</sup> and molecular rotors.<sup>12–14</sup>

We previously reported the synthesis and physicochemical characterization of benchmark macrocycle **1** and BODIPY-phenylacetylene macrocycle **2a** (Fig. 1).<sup>15</sup> By combining the well-studied BODIPY dye systems<sup>16–20</sup> with phenylacetylene architectures we had hoped to develop supramolecular-inspired organic dyes for dye-sensitised solar cell applications.<sup>21–24</sup> Particularly, we were interested in designing novel  $\pi$ -spacers that could be

exploited for panchromatic absorption within the DSSC manifold. Curiously, we thought that if we could use the phenylacetylene macrocycle as an antenna, then we could effectively harvest more light. In our previous report we observed energy transfer from the macrocycle ( $\lambda_{\text{ex}} = 292$  nm) to the BODIPY core (quantum yield of 0.89) as the fluorescence emanated from the BODIPY.<sup>15</sup> However, the absorption profile of the macrocycle lied predominantly in the UV region, ultimately preventing the use of this molecule architecture for terrestrial photovoltaic applications. To address this limitation, we sought to red-shift the absorption profile of the macrocycle and attempted to further increase the efficiency of the energy transfer process by altering the rigidity and orthogonality of the BODIPY core. Initially we tried to modify the phenylacetylene-macrocycle by putting electron donating group (EDG, *e.g.*, –OMe) and electron withdrawing group (EWG; *e.g.*, –NO<sub>2</sub>) as shown in Fig. 1. However, because of synthetic challenges we were unable to add EWGs on the macrocycle and decided to explore EDGs only. Herein, we report the synthesis and physicochemical characterization of di- and tetramethoxy substituted phenylacetylene-BODIPY macrocyclic dyads **2b–d** (Scheme 1), as well as the more rigid **2e** dyad containing a tetra-methylated BODIPY core.

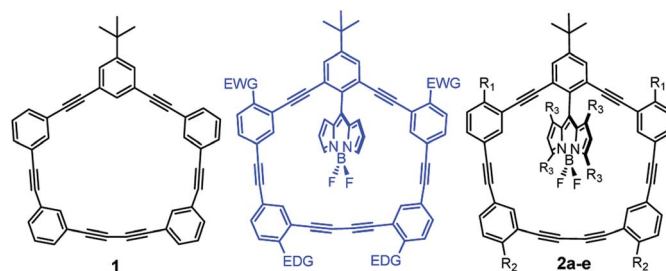


Fig. 1 BODIPY-phenylacetylene macrocycles in this study. **2a** ( $R_1 = R_2 = R_3 = \text{H}$ ), **2b** ( $R_1 = R_3 = \text{H}$ ;  $R_2 = \text{OCH}_3$ ), **2c** ( $R_1 = \text{OCH}_3$ ;  $R_2 = R_3 = \text{H}$ ), **2d** ( $R_1 = R_2 = \text{OCH}_3$ ;  $R_3 = \text{H}$ ), **2e** ( $R_1 = R_2 = -\text{H}$ ;  $R_3 = -\text{CH}_3$ ).

<sup>a</sup>Department of Chemistry and Biology, Ryerson University, 350 Victoria St, Toronto, Canada. E-mail: bryan.koivisto@ryerson.ca

<sup>b</sup>Institute of Chemistry, University of the Punjab, Quaid-i-Azam Campus, Lahore-54590, Pakistan

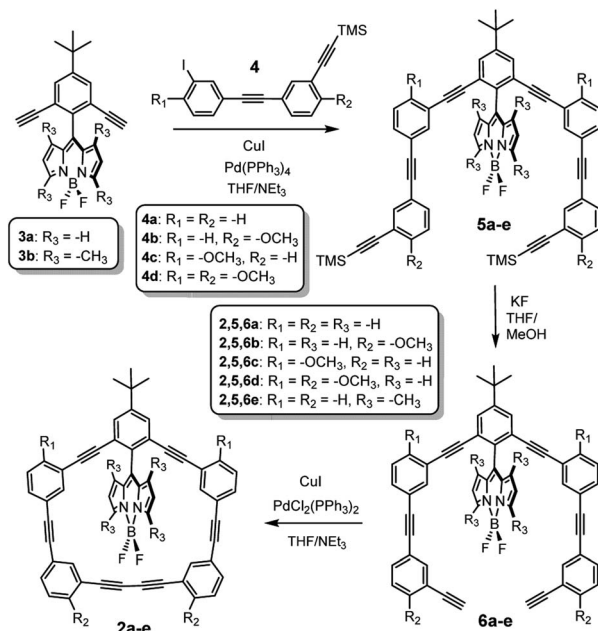
<sup>c</sup>Instituto de Ciencias Químicas Aplicadas, Facultad de Ingeniería, Universidad Autónoma de Chile, Llano Subercaseaux 2801, Santiago, Chile

<sup>d</sup>Departamento de Química Inorgánica, Facultad de Química, Pontificia Universidad Católica de Chile. Avda. Vicuña Mackenna 4860, Santiago, Chile

<sup>e</sup>Department of Chemistry, University of Toronto, Toronto, Canada

† Electronic supplementary information (ESI) available. CCDC 1836414 and 1836415. For ESI and crystallographic data in CIF or other electronic format see DOI: 10.1039/c8ra03384f





Scheme 1 Synthesis of BODIPY-phenylacetylene macrocycles **2a–2e**.

## Synthesis and characterization

The synthesis of the control macrocycle **1** and BODIPY-macrocycle **2a** have been previously reported,<sup>15</sup> and the general synthetic route leading to **2b–e** is depicted in Scheme 1. Sonogashira cross-coupling reaction between BODIPY **3a–b** and TMS-protected acetylenes **4a–d** yielded **5b–e**, which were subsequently deprotected with KF to afford **6b–e**. BODIPY macrocycles **2b–e** were obtained *via* oxidative, Glazer-like cross-coupling using PdCl<sub>2</sub>(PPh<sub>3</sub>)<sub>2</sub> and CuI.

Complete experimental details and characterization can be found in the ESI, but as expected, the <sup>1</sup>H, <sup>13</sup>C, <sup>11</sup>B and <sup>19</sup>F NMR spectra reveal numerous similarities between the five BODIPY-phenylacetylene macrocycles, as well as supporting their proposed structures. The structural identity of **2b** and **2c** was further confirmed using X-ray crystallography (Fig. 2) as needles were grown *via* slow evaporation of saturated dichloromethane/hexanes (2 : 1). Despite the presence of the donating methoxy groups at different locations in the molecule, little structural differences are observed when considering key bond lengths and angles (tabulated in Table 1). In both compounds, the phenylacetylene macrocycle is planar and the BODIPY is canted relative to this phenylacetylene macrocyclic plane (see dihedral angle). It was hoped that the donating group would attenuate the bond lengths more, but both structures possess similar bond lengths and angles, and the -OMe group does little to alter the solid state structure. Unfortunately, the crystal structure of **2d** was never obtained because the tiny needle-like crystals were prone to solvent loss and cracking.

## Results and discussion

To better appreciate the effect of adding electron donating groups around the periphery of the macrocycles, optical

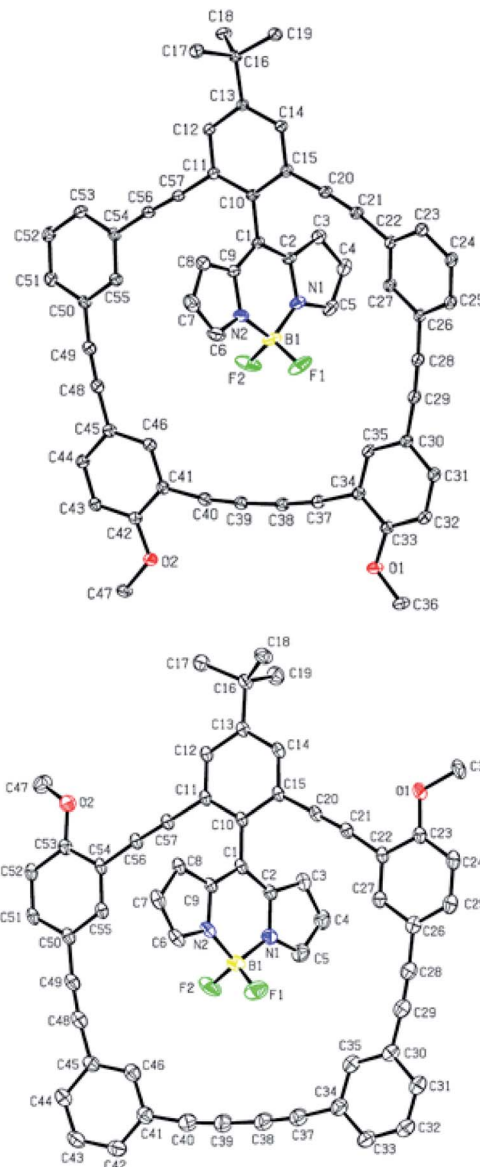


Fig. 2 Crystal structures of **2b** (top) and **2c** (bottom); ORTEP, 30% thermal ellipsoids. Hydrogen atoms and solvent molecules were removed for clarity.

measurements (absorption/fluorescence) were performed and correlated to theoretical calculations. The spectra of compounds **2b–e** (in DCM) have been presented in Fig. 3–6 respectively, and they have been contrasted to benchmark **2a**. In addition, fluorescence emission is depicted for  $\lambda_{\text{exc}}$ , and in all cases emission emanates from the BODIPY. The presence of -OMe groups on the macrocycle (**2b–d**) only modestly effects the absorption profile (between 330–380 nm) of these dyads, and specific comparisons relating to this lower energy absorption shoulder (belonging to the phenylacetylene macrocycle) are collated in Table 2.

Fig. 3 shows the photophysical behaviour for compound **2b**; a more detailed TD-DFT assignment for **2b** can be found in Table S2 (ESI†). A closer examination of Fig. 3 reveals that when



Table 1 Select bond angles and distances from Fig. 2<sup>a</sup>

Dyad	Distance (C45–C50)	Distance (C34–C41)	Distance (C26–C30)	Dihedral angle C15–C10–C1–C9
<b>2b</b>	4.048	6.572	4.050	117.0
<b>2c</b>	4.067	6.552	4.043	116.5

<sup>a</sup> Bond lengths/distance have been reported above in Angstroms.

Table 2 Photophysical data for low energy shoulder (330–380 nm) of **2a–e**<sup>a</sup>

Dye	Absorption <sup>b</sup>			Fluorescence		
	$\lambda_{\max}$ (nm)	$(\epsilon \times 10^4 \text{ LM}^{-1} \text{ cm}^{-1})$	TD-DFT assignment <sup>c</sup>	$\lambda_{\text{em}}$ (nm)	$\phi^d$	ETE <sup>e</sup> (%)
<b>2a</b>	338	3.60	HOMO – 1 to LUMO + 3	528	0.89	>95
<b>2b</b>	364	2.65	HOMO to LUMO + 1	527	0.84	~70
<b>2c</b>	337	4.70	HOMO – 3 to LUMO + 1	530	0.85	>95
<b>2d</b>	376	2.64	HOMO to LUMO + 1	533	0.81	~70
<b>2e</b>	335	3.12	HOMO – 5 to LUMO	521	0.91	~90

<sup>a</sup> More detailed theoretical assignments are found in the ESI. <sup>b</sup> Low energy phenylacetylene absorption shoulder for **2a**, **2b**, **2c**, **2d** and **2e** in DCM. <sup>c</sup> Assigned FMO transitions based on TDDFT (B3LYP/6-31G) calculations. <sup>d</sup> Measurements were made in DCM (dichloromethane). Quantum yield calculated at 22 °C relative to Rhodamine 6G (QY = 0.95). <sup>e</sup> Energy transfer efficiency (ETE) calculated based on integrating the emission profile and comparing the high and low energy emission (from excitation at ~300 nm).

contrasted to **2a**, the phenylacetylene shoulder is red-shifted to 364 nm; otherwise the two spectra share many of the same features. This absorption has been assigned to the HOMO to LUMO + 1 transition, which is heavily centred on the  $\pi$ -system proximal to the –OMe groups. While, excitation at 364 nm resulted in BODIPY emission with a Stokes shift of 163 nm, the energy transfer is not quantitative, as there is a solvent-dependent fluorescence (see ESI Fig. 74<sup>†</sup>) centred at 400 nm.

Fig. 4 shows the optical properties for compound **2c**; a more detailed TD-DFT assignment for **2c** can be found in Table S3 (ESI<sup>†</sup>). When contrasted to **2a**, the macrocycle profile is nearly identical, with the presence of an inflection point at 315 nm. This absorption shoulder has been assigned to the HOMO – 3

to LUMO + 1 transition, where electron density of the HOMO – 3 is heavily centred on the  $\pi$ -system distal to the –OMe groups. As a result, the methoxy groups do little to perturb the energetics of the involved orbitals, and the energy transfer efficiency resembles that of **2a**.<sup>15</sup>

Fig. 5 depicts the absorption and emission behaviour for compound **2d**; a more detailed TD-DFT assignment for **2d** can be found in Table S4 (ESI<sup>†</sup>). When contrasted with **2a**, it is now possible to see more substantive differences in the absorption profile of **2d**. Although modest, the addition of distal and proximal methoxy groups red-shifts the high energy region of the absorption profile by 8 nm (292 nm for **2a** to 300 nm for **2d**) resembling the superposition of what is observed in **2b** and **2c**. The lowest energy macrocycle transition has again been

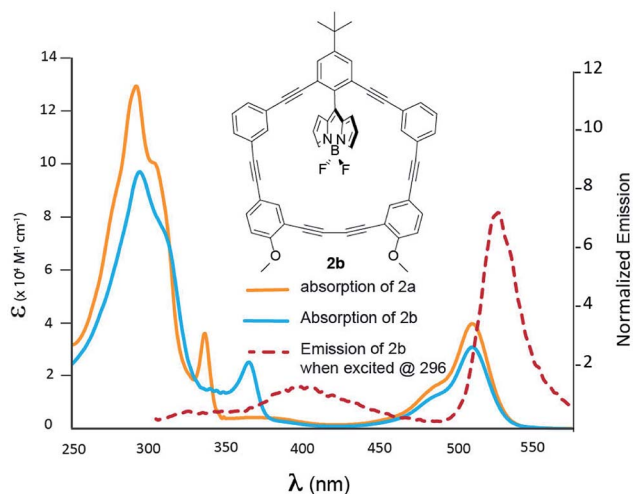


Fig. 3 Absorption spectra of **2a** (blue) and **2b** (orange) recorded in DCM. Emission of **2b** is presented by the dashed red line.

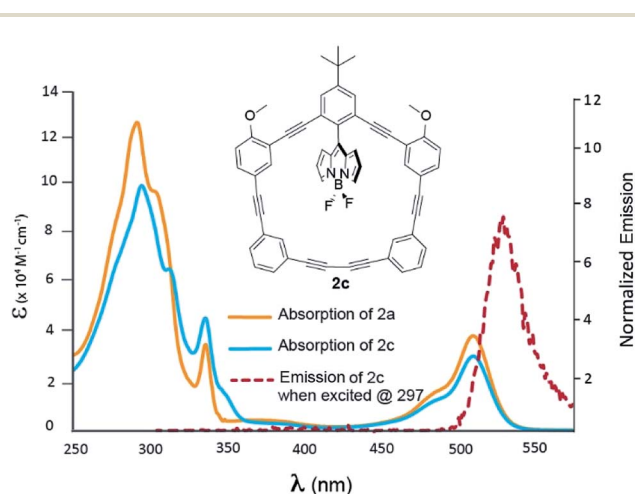


Fig. 4 Absorption spectra of **2a** (blue) and **2c** (orange) recorded in DCM. Emission of **2c** is presented by the dashed red line.



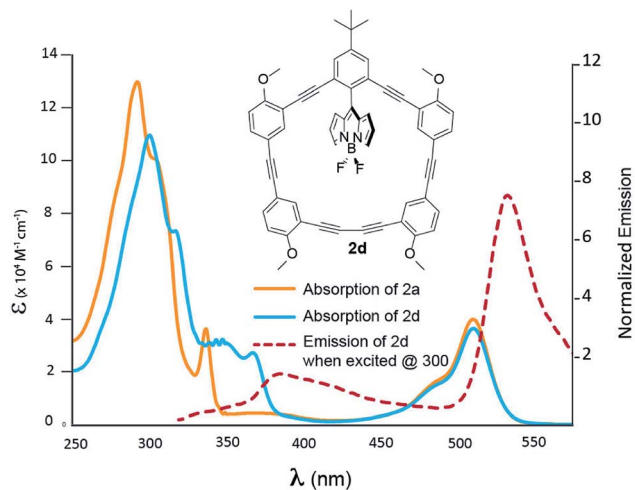


Fig. 5 Absorption spectra of **2a** (blue) and **2d** (orange) recorded in DCM. Emission of **2d** is presented by the dashed red line.

assigned to the HOMO to LUMO + 1 transition, where the HOMO now has a greater degree of delocalization throughout the macrocycle  $\pi$ -system. In this instance, the  $-OMe$  groups raise the HOMO energy which ultimately red-shifts the absorption spectrum. Again, excitation at 376 nm resulted in BODIPY emission with a Stokes shift of 157 nm. Another observation to note (from Table 2) is that as  $-OMe$  groups are added to the macrocycle, there is a decrease in the quantum yield, and as with **2b**, a solvent dependent fluorescence is observed. This is consistent with the notion that increased degrees of freedom, should lead to more non-radiative pathways that would ultimately decrease fluorescence intensity.

Fig. 6 shows the photophysical behaviour for compound **2e**; a more detailed TD-DFT assignments for **2e** can be found in Table S5 (ESI<sup>†</sup>). This particular dyad does not have  $-OMe$  groups attached, and as such it is an outlier when considering macrocycle modification, but it was designed to determine if increased rigidity of the BODIPY within the macrocycle would result in altered absorption, energy transfer or emissive

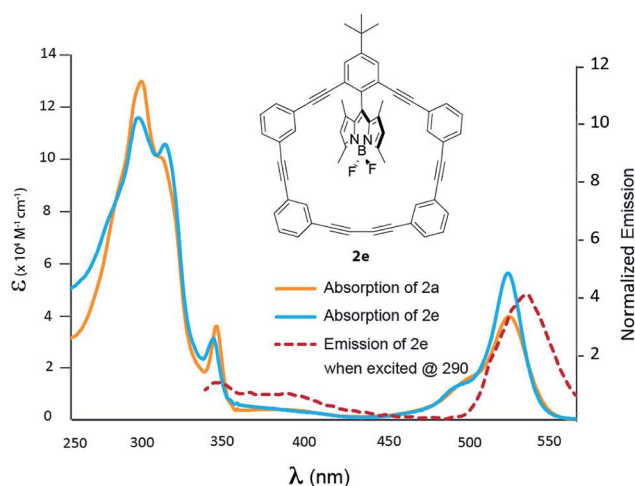


Fig. 6 Absorption spectra of **2a** (blue) and **2e** (orange) recorded in DCM. Emission of **2e** is presented by the dashed red line.

behaviour. At first glance, the high energy absorption is nearly identical to **2a** (the non-methylated BODIPY) with a slight difference in relative extinction coefficients. This would be expected as tuning the orthogonal BODIPY should have little impact on the macrocycle absorption. Curiously, the extinction coefficient owing to the BODIPY transition (at 530 nm) increases nearly 40% compared to **2a**. The efficiency of the energy transfer is difficult to gauge (and theoretical calculations can be found in the ESI<sup>†</sup>), but having methyl groups attached to the BODIPY was designed to 'stuff it' in the macrocycle and minimize canting/rotational degrees of freedom – which may mitigate through-bond exchange owing to increase orthogonality between the macrocycle and BODIPY. The low energy macrocycle shoulder was assigned as a HOMO – 5 to LUMO transition, and excitation at 335 nm leads to a BODIPY emission with an increased quantum yield (Table 2), and a Stokes shift of 188 nm.

## Conclusions

Four novel BODIPY-phenylacetylene macrocycles (**2b–e**) were synthesized and their photophysical behaviour contrasted with the previously reported benchmark **2a**. With the intent of red-shifting the absorption profile of the macrocycle using strong resonance donors (*i.e.*,  $-OMe$  groups), it was revealed that modification of the BODIPY-phenylacetylene framework does lead to bathochromically shifted absorption spectra. While the effect was modest, this strategy still exhibited the desired energy transfer (from the macrocycle to the BODIPY core), with only a slight decrease in fluorescence quantum yield when  $-OMe$  groups were added distal to the BODIPY (**2b**, **2d**). This work also suggests that modifying the macrocycle and simultaneously rigidifying the BODIPY within the macrocyclic cavity (as seen with **2e**) could be a strategy employed to mitigate the losses in quantum yield while maintaining the desired bathochromic shift. Still many questions remain about the nature (rates, Dexter *vs.* Forster, *etc.*) of the energy transfer. However, outfitted with this family of macrocyclic dyads, further structure–property insights regarding these questions could be obtained with the appropriate collaboration. Furthermore, the design of a [2]-rotaxane analogue where only Forster energy transfer is possible, would also garner unique energy transfer insights, and this will be articulated in future work.

## Conflicts of interest

There are no conflicts to declare.

## Acknowledgements

BDK would like to acknowledge NSERC & Ryerson University for their financial support. ESV and XZB would like to acknowledge, Fondap/serc chile/15110019 and Fondecyt 1161416 and 1180565, respectively.



## Notes and references

- 1 N. Aratani, D. Kim and A. Osuka, *Acc. Chem. Res.*, 2009, **42**, 1922–1934.
- 2 J. Yang, M.-C. Yoon, H. Yoo, P. Kim and D. Kim, *Chem. Soc. Rev.*, 2012, **41**, 4808–4826.
- 3 K. Nakao, M. Nishimura, T. Tamachi, Y. Kuwatani, H. Miyasaka, T. Nishinaga and M. Iyoda, *J. Am. Chem. Soc.*, 2006, **128**, 16740–16747.
- 4 M. Iyoda, J. Yamakawa and M. J. Rahman, *Angew. Chem., Int. Ed.*, 2011, **50**, 10522–10553.
- 5 S. Campagna, F. Puntoriero, F. Nastasi, G. Bergamini and V. Balzani, *Top. Curr. Chem.*, 2007, **280**, 117–214.
- 6 T. Pullerits and V. Sundstrom, *Acc. Chem. Res.*, 1996, **29**, 381–389.
- 7 A. W. Roszak, T. D. Howard, J. Southall, A. T. Gardiner, C. J. Law, N. W. Isaacs and R. J. Cogdell, *Science*, 2003, **302**, 1969–1972.
- 8 D. Venkataraman, S. Lee, J. S. Zhang and J. S. Moore, *Nature*, 1994, **371**, 591–593.
- 9 Y. Hosokawa, T. Kawase and M. Oda, *Chem. Commun.*, 2001, 1948–1949.
- 10 M. A. Reed, M. J. Chen, A. M. Rawlett, D. W. Price and J. M. Tour, *Appl. Phys. Lett.*, 2001, **78**, 3735–3737.
- 11 J. M. Tour, M. Kozaki and J. M. Seminario, *J. Am. Chem. Soc.*, 1998, **120**, 8486–8493.
- 12 T. R. Kelly, *Acc. Chem. Res.*, 2001, **34**, 514–522.
- 13 D. Moessinger, J. Hornung, S. Lei, S. De Feyter and S. Hoeger, *Angew. Chem., Int. Ed.*, 2007, **46**, 6802–6806.
- 14 G. S. Kottas, L. I. Clarke, D. Horinek and J. Michl, *Chem. Rev.*, 2005, **105**, 1281–1376.
- 15 M. Yousaf, A. J. Lough, E. Schott and B. D. Koivisto, *RSC Adv.*, 2015, **5**, 57490–57492.
- 16 A. Loudet and K. Burgess, *Chem. Rev.*, 2007, **107**, 4891–4932.
- 17 G. Ulrich, R. Ziessel and A. Harriman, *Angew. Chem., Int. Ed.*, 2008, **47**, 1184–1209.
- 18 R. Ziessel and A. Harriman, *Chem. Commun.*, 2011, **47**, 611–631.
- 19 E. Heyer and R. Ziessel, *J. Org. Chem.*, 2015, **80**, 6737–6753.
- 20 J. Banuelos, *Chem. Rec.*, 2016, **16**, 335–348.
- 21 C. Bonnier, D. D. Machin, O. Abdi and B. D. Koivisto, *Org. Biomol. Chem.*, 2013, **11**, 3756–3760.
- 22 S. Erten-Ela, M. D. Yilmaz, B. Icli, Y. Dede, S. Icli and E. U. Akkaya, *Org. Lett.*, 2008, **10**, 3299–3302.
- 23 S. Kolemen, O. A. Bozdemir, Y. Cakmak, G. Barin, S. Erten-Ela, M. Marszalek, J. H. Yum, S. M. Zakeeruddin, M. K. Nazeeruddin, M. Gratzel and E. U. Akkaya, *Chem. Sci.*, 2011, **2**, 949–954.
- 24 A. Bessette and G. S. Hanan, *Chem. Soc. Rev.*, 2014, **43**, 3342–3405.

